Supplementary Information (SI) for Nanoscale.

Determination of Carrier Temperature in Weakly Confined Semiconductors Using Time-Resolved Optical Spectroscopy: Supporting Information

Ivo Tanghe,[†,‡,¶] Chao-Yang Lin,[§,‖] Isabella Wagner,[§,‖] Margarita Samoli,[‡] Servet Ataberk Cayan,[‡,¶] Zeger Hens,[‡,¶] Justin Hodgkiss,[§,‖] Kai Chen,[⊥,‖,#] and Pieter Geiregat[*,‡,¶]

†*Photonics Research Group, Ghent University, Belgium*

‡*Physics and Chemistry of Nanostructures, Ghent University, 9000 Ghent, Belgium*

¶*NoLIMITS Center for Non-Linear Microscopy and Spectroscopy, Ghent University, 9000 Ghent, Belgium*

§*School of Chemical and Physical Sciences, Victoria University of Wellington, Wellington, New Zealand*

‖*MacDiarmid Institute for Advanced Materials and Nanotechnology, New Zealand.*

⊥*Robinson Research Institute, Victoria University of Wellington, Wellington, New Zealand*

#*The Dodd-Walls Centre for Photonic and Quantum Technologies, University of Otago, Dunedin, New Zealand*

E-mail: pieter.geiregat@ugent.be

S1 Materials

S1.1 Synthesis and Characterization

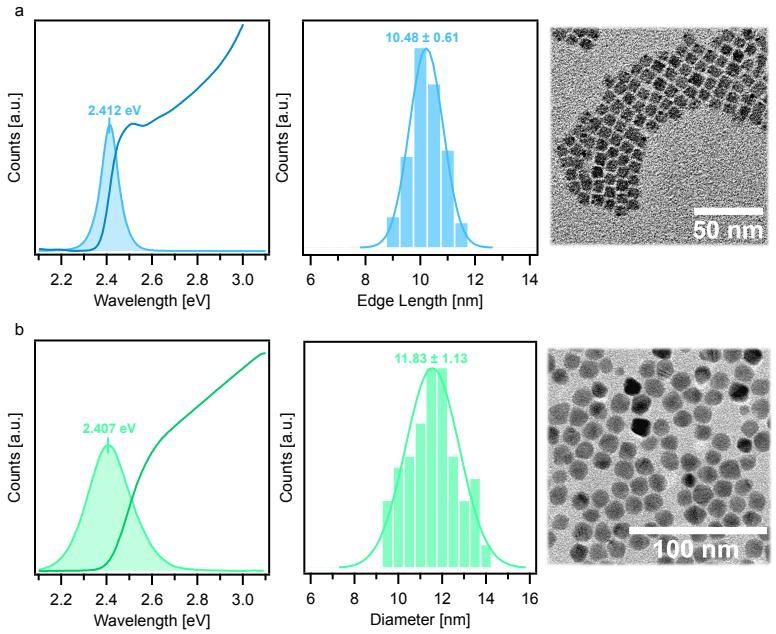

Figure S1: Absorption, PL, TEM sizing histogram and TEM imaging of the (a) perovskite $CsPbBr_3$ and (b) wurtzite CdS nanocrystals used in this work.

S1.1.1 $CsPbBr_3$

For the synthesis of the 10 nm CsPbBr3 nanoparticles, a modified version of the protocol reported by Baranov et al. was used.[1]

Perovskite precursors Cesium carbonate (Cs_2CO_3, 99.9% trace metals basis) was purchased from Sigma Aldrich. Lead bromide ($PbBr_2$, Puratronic 99.999% metals basis) was purchased from Alfa Aesar. Oleic acid (OA, technical grade 90%), oleylamine (OLA, approx. C_{18}-content 80-90%) and 1-octadecene (1-ODE, technical grade 90%) were purchased from Thermo Fischer Scientific and further distilled. Anhydrous toluene (99.9% Extra dry, AcroSeal) and anhydrous acetone (99.9% Extra dry, AcroSeal) were purchased from Thermo

Fischer Scientific and used as is. All chemicals were stored in N_2-filled gloveboxes until further use.

For the Cs-oleate solution (0.07 M), 400 mg of cesium carbonate (1.23 mmol), 1.75 mL of OA and 15 mL of 1-ODE were loaded into a 25 mL three-neck flask. The flask was degassed for 1h at 105 °C and then heated under nitrogen to 120 °C until the cesium carbonate fully dissolved (around 30 min). Since the stock solution turns turbid at room T, it was gently heated at 100 °C before use.

Synthesis The following reaction mix was prepared in the glovebox. In a 20 ml vial, 73 mg $PbBr_2$ (0.20 mmol), 0.5 ml OLA, 0.05 ml OA and 5 ml 1-ODE were added. The vial was then equipped with a stirring bar and closed with a septum screw cap before bringing out. Once outside the glovebox, the vial was attached to a nitrogen-filled Schlenk line with the help of a needle and tube. Once the vial was placed under a continuous N_2 flush, a thermocouple was inserted into the solution through the septum cap. The vial was then fixed inside an aluminum block that was placed onto a pre-heated stirring plate at 180 °C. The solution was left to heat up for around 20 min until the reactants fully dissolved. As soon as the solution had no visible traces of undissolved salts, the vial was lifted and placed on top of the block while still under stirring. As the vial naturally cooled down, once the temperature reached 170 °C, 0.5 ml of the Cs-oleate solution were swiftly injected. At this stage the contents of the vial should turn clear yellow, then turbid bright green as the vial is left to naturally cool down to room T.

For the purification, the stirring bar was removed and the vial was then centrifuged at 4000 rpm for 5 min. The resulting surnatant was discarded and the vial containing the bright yellow precipitate was centrifuged once again at 4000 rpm for an additional 3 min. The remaining surnatant fraction was carefully removed with the help of a cotton swap and the sides of the vial were wiped with a lint-free tissue. The particles were then re-dispersed in 1 ml of toluene. The stirring bar was added again, along with 35 µL of OLA and OA

each in order to prevent degradation of the particles with the addition of polar solvents. Then, under constant stirring, around 1.5 ml of anhydrous acetone were added in a dropwise manner until the solution turned turbid. The vial was then finally centrifuged for 5 min at 5000 rpm and the resulting precipitate was re-dispersed in 1 ml toluene, giving a clear bright green final sample.

S1.1.2 CdS

For the synthesis of the 12 nm CdS nanoparticles, a modified version of the protocol reported by Tanghe et al. was used as described below.[2]

CdS Precursors Cadmium oxide (CdO, 99.5%), toluene (C_7H_8, 99.9%), methanol (CH_3OH, 99.8%) and 2-propanol (C_3H_8O, 99.8%) were purchased from Chemlab Analytical. Tri-n-octylphosphine ($C_{24}H_{51}P$, min. 97%) was purchased from Strem Chemicals. Elemental sulfur ($S > 99.5\%$) was purchased from Sigma Aldrich. 1-octadecane ($C_{18}H_{38}$, tech. 90%) and oleic acid ($C_{18}H_{34}O_2$, tech. 90%) were purchased from Thermo Fisher Scientific. All chemicals were used as is with no further purifications.

For the Cd-oleate solution (0.50 M), 1.024 g CdO (8 mmol), 8 mL of oleic acid and 8 mL of 1-octadecane were added into a 50 mL three-necked flask. The flask was put under vacuum and then degassed for 60 min at 110 °C. Next, the flask was filled with N_2 and heated to 300 °C where it was left for approximately 5 min until the reactants complexed and the mixture turned clear. The obtained solution was then cooled down to room temperature and stored in a 20 ml vial. Since the oleate precursor solidifies upon cooling, it should be gently heated at 100 °C before use. The TOP-S solution (0.50 M) was prepared by adding 10 mL TOP and 0.160 g of S (5 mmol) in a 20 ml vial under N_2. The solution was stirred at 90 °C for 30 minutes until fully complexed and turned clear. Both precursors were stored in nitrogen-filled gloveboxes until further use.

Synthesis of 12 nm CdS Nanoparticles In a 50 mL three-neck flask, 8 mL of 1-octadecane were added and degassed for 60 min at 110 °C. Afterwards, the flask was filled with N_2 and heated to 320 °C. In the meantime, an equimolar solution of Cd-oleate and TOP-S was pre-mixed and slowly injected into the flask at a 2 mL/hour rate under stirring. The total injection time is adjusted accordingly to synthesize the desired size each time. For example, in order to obtain 12 nm cores, a total of 1.25 ml Cd-oleate and 1.25 ml TOP-S were mixed and injected over the course of 75 min. At the end of the injection, the reaction medium was left undisturbed at 320 °C for an additional 45 min to allow the remaining precursors to fully react and promote size focusing/ripening of any smaller particles.

Afterwards, the reaction was cooled down to room temperature and underwent a purification cycle. This included splitting the crude mix into four centrifugation tubes and adding 15 ml of a 2:1 ratio mix of 2-propanol and methanol in each tube. The particles were then crashed by centrifuging at 5000 rpm for 10 min. This process was repeated for a total of two purification steps. After the purification was complete, the particles were re-dispersed in 3 ml toluene for further use.

S1.2 Optical Properties

S1.2.1 Intrinsic Absorption of $CsPbBr_3$

For the halide perovskite $CsPbBr_3$ we refer to the paper of Maes et al.[3] who deduced the intrinsic absorption coefficient through combined optical and analytical methods as given in *n*-hexane:

$$\mu_{i,0}(335\text{ nm}) = 1.5910^5\text{ cm}^{-1} \tag{S1}$$

Using this value, one can normalize the absorption spectrum of the $CsPbBr_3$ perovskite nanocrystals dispersed in n-hexane, as shown in Figure S1. From this we can calculate for example for the ca. 12 nm NCs a cross section using $\sigma = \mu_{i,0}V$ with V the volume of the nanocrystal.[4]

S1.2.2 Intrinsic Absorption of wz-CdS

To calculate the intrinsic absorbance, we start from the dielectric constants of wurtzite CdS from Adachi *et al.*, for a wavelength of 300 nm. Due to the assymmetric nature of the crystal and the random orientation, we can average out the dielectric constant for electrical fields parallel and perpendicular to the *c*-axis

$$\tilde{\epsilon} = \frac{1}{3}\cdot\underbrace{(6.663 + 3.623i)}_{E\perp c} + \frac{2}{3}\cdot\underbrace{(6.601 + 3.466i)}_{E\parallel c} = 6.6217 + 3.5183i \tag{S2}$$

From which we can calculate the intrinsic absorbance

$$\mu_i = \frac{2\pi}{\lambda n_s}\cdot\Im(\tilde{\epsilon})\cdot|f_{LF}|^2 \tag{S3}$$

Where n_s the refractive index of the solvent, λ the wavelength at which we calculate the intrinsic absorbance (here we will use 300 nm, as stated above), and $|f_{LF}|^2$ the squared

local-field factor, defined as (assuming here spherical particles):

$$f_{LF} = \frac{3 \cdot \epsilon_s}{\tilde{\epsilon} + 2 \cdot \epsilon_s} \tag{S4}$$

With ϵ_s the dielectric constant for toluene, we find a value for the intrinsic absorbance

$$\mu_i(300 \text{ nm}) = 1.82 \times 10^5 \text{ cm}^{-1} \tag{S5}$$

Knowing that at short wavelengths the absorbance spectrum becomes size independent, we can use this value to determine the wavelength-dependent intrinsic absorbance

$$\mu_i(\lambda) = \frac{A_0(\lambda)}{A_0(300 \text{ nm})} \cdot \mu_i(300 \text{ nm}) \tag{S6}$$

From this we can calculate for example for the 12.1 nm BNCs a cross section series at 400 and 480 nm: $\sigma(400 \text{ nm}) = 7.3510^{-14}$ cm^2 and $\sigma(480 \text{ nm}) = 3.810^{-14}$ cm^2. To generate a single electron-hole pair in a 12.1 nm BNC, one would hence need 6.7 µJ/cm^2 and 11 µJ/cm^2 at 400 and 480 nm respectively.

S2 Experimental Methods

S2.1 Transient Absorption Spectroscopy

Samples were excited using 110 femtosecond pump pulses at 400 nm, through second harmonic generation in alpha-BBO. Probe pulses were generated in a 1 mm thick CaF_2 crystal using the 800 nm fundamental. The pulses were delayed relative to the pump using a delay stage with maximum delay of 3 ns for 400 nm pumping. The probe spectrum in our experiments covers the UV-VIS window from 420 nm up to 700 nm. The quantum dots were dispersed in an optically transparent solvent (toluene) and continuously stirred to avoid charging or photo-degradation. The pump wavelength and sample concentration were chosen to obtain an optimal trade-off between having a good signal at the band-edge transitions, while still not having a too strong absorption at the pump-wavelength as to assure a uniform pumping of the sample.

The average number of absorbed photons (or equivalently created excitons) at time zero, noted as $\langle N \rangle$, can be calculated from the photon flux J_{ph}, the cuvette length L and the nanocrystal absorption cross section at the pump wavelength σ_{λ_p}: $\langle N \rangle = J_{ph} \times \sigma_{\lambda_p} \times \frac{1-e^{-\alpha_{0,\lambda_p} L}}{\alpha_{0,\lambda_p} L}$. The photon flux is calculated from the beam area, obtained through a Thorlabs CCD beam profiler, and defined as $A_{beam} = 2\pi \times \sigma_x \sigma_y$ where σ_i is the standard deviation in the $i = x, y$ direction. Note that the carrier density n follows as $\langle N \rangle / V$, with V the volume of the nanocrystal.

S2.2 Femtosecond Photoluminescence Spectroscopy

For the detection of the broadband PL transients on a sub-picosecond timescale, we used the transient grating PL technique.[5] The output of a femtosecond Ti:S laser was split into pump and gate parts. For the pump part, second harmonic (400 nm) generation was used in the experiments and focused to a 50 μm^2 spot onto the sample. During the measurement, the sample was continuously stirred in a 1 mm cuvette to avoid photo-induced degradation

effects or charging of the nanoparticles. The PL signal from the sample was collected and refocused onto the gate medium, a 1 mm fused silica crystal, using a pair of off-axis parabolic mirrors. For the gate part, about 40 µJ of the 800 nm output was split using a 50/50 beam splitter to generate the two gate beams and focused onto the gate medium at a crossing angle of approximately 8 degrees and overlapped with the PL in a boxcar geometry. The two gate beams, which spatial and temporal overlap inside the gate medium, generate a laser-induced grating. This transient grating acts like an ultrafast optical shutter to temporally resolve the broadband PL signals by diffracting the gated signal from the PL background. Two achromatic lenses collimated and focussed the gated signals onto the spectrometer entrance (Princeton Instruments SP 2150), and the gated PL spectra were measured by an intensified CCD camera (Princeton Instruments, PIMAX3). The time delay between pump and gate beams was controlled via a motorized optical delay line. For each transient PL spectrum, 120 000 shots at each gate time delay were accumulated.

S2.3 Carrier Density

The carrier density n is calculated based on Poissonian statistics and is defined as: $n = \frac{\langle N \rangle}{V_{QD}}$. Here , $\langle N \rangle$ describes the mean of a Poissonian distribution used to model the light absorption in an ensemble of nanoparticles as a series of random events. Such models are widely used in the context of nanocrystals, with the small semantic difference that $\langle N \rangle$ then often refers to "excitons" and not unbound electron-hole pairs, yet this makes no difference in the use of the expression. $\langle N \rangle$ can be calculated from the photon flux J_{ph} (in photons/cm^2) and the cross section for absorption, see section 1.4 above: $\langle N \rangle = J_{ph} \times \sigma$.

S2.4 Raw Data for Temperature Determination

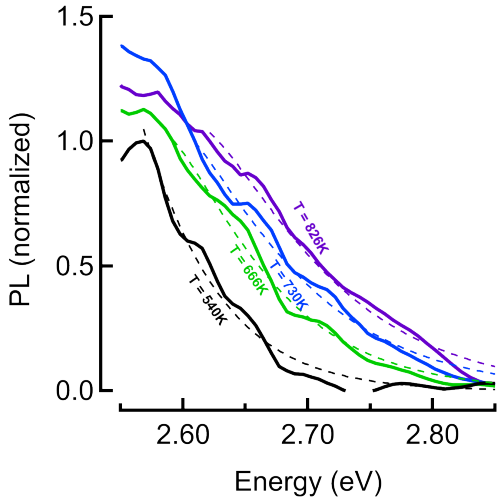

Figure S2: PL emission at high photon energy at 3 ps time delay of CdS nanocrystals after 400 nm excitation.

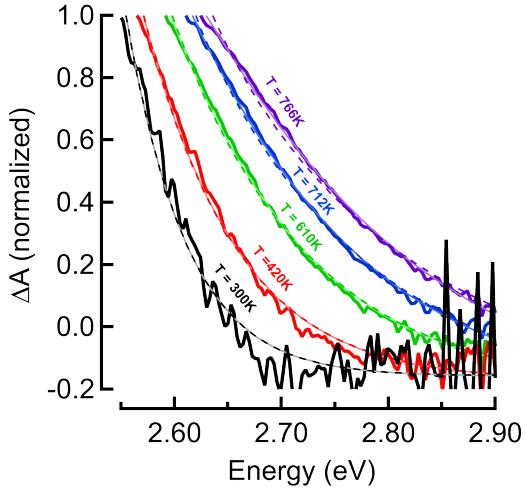

Figure S3: TA spectra at high photon energy at 3 ps time delay of CdS nanocrystals after 400 nm excitation.

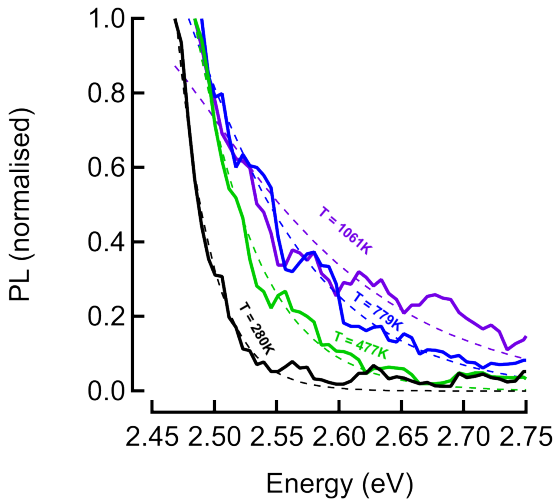

Figure S4: PL emission at high photon energy at 3 ps time delay of perovskite nanocrystals after 400 nm excitation.

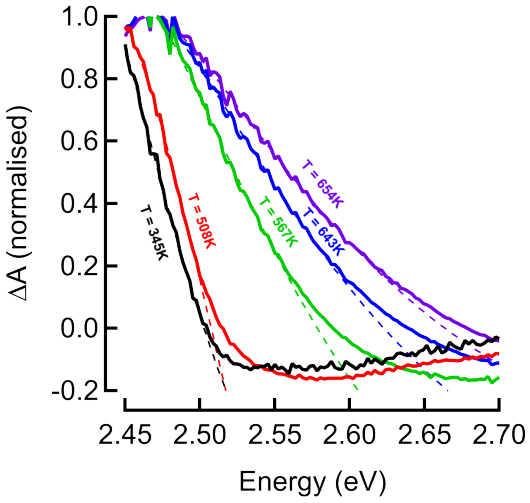

Figure S5: TA spectra at high photon energy at 3 ps time delay of perovskite nanocrystals after 400 nm excitation.

S3 Theory Model

S3.1 Transient Absorption

We start from the idea that A can be written as

$$A(E,T) = A_0(E,T) \times (f_h(E,T) - f_e(E,T)) \tag{S7}$$

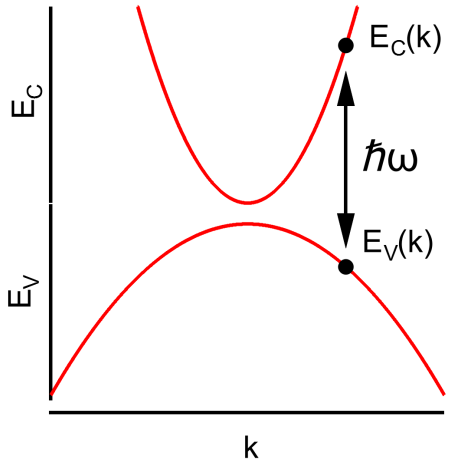

Figure S6: Asymmetrical simple bandstructure used to derive the theory in the paper.

where $f_h(E,T), f_e(E,T)$ are defined as

$$f_e(E,T) = \frac{1}{1+\exp\left(\frac{E_C(k)-E_{F,e}}{k_BT}\right)} \tag{S8}$$

$$f_h(E,T) = \frac{1}{1+\exp\left(\frac{E_V(k)-E_{F,h}}{k_BT}\right)} \tag{S9}$$

which are the occupation chances of electrons in the conduction - and valence band respectively. $E_C(k)$ and $E_V(k)$ are energy dependent through the carrier momentum k. We can calculate the quasi fermi levels back from the carrier density n. The selection rule for an absorption event is that there cannot be any momentum change when absorbing a photon with frequency ω, so the relationship $\hbar\omega = E = E_C(k) - E_V(k)$ holds, with

$$E_C(k) = E_g + \frac{\hbar^2 k^2}{2m_e^*} \tag{S10}$$

$$E_V(k) = -\frac{\hbar^2 k^2}{2m_h^*} \tag{S11}$$

where m_e^* and m_h^* are the effective masses of the electrons and holes, respectively. From this we can calculate

$$E = E_g + \frac{\hbar^2 k^2}{2m_e^*} + \frac{\hbar^2 k^2}{2m_h^*} = E_g + \frac{\hbar^2 k^2}{2m_r} \tag{S12}$$

with m_r the reduced effective mass $\left(\frac{1}{m_e^*} + \frac{1}{m_h^*}\right)^{-1}$. Solving this for k, we get

$$k_0 = \sqrt{\frac{2m_r}{\hbar^2}(E - E_g)} \tag{S13}$$

If we combine the selection rules with the FD occupation factors, we find

$$f_e(E,T) = \frac{1}{1 + \exp\left(\dfrac{E_g + \frac{\hbar^2 k_0^2}{2m_e^*} - E_{F,e}}{k_B T}\right)} = \frac{1}{1 + \exp\left(\dfrac{E_g + \frac{m_r}{m_e^*}(E - E_g) - E_{F,e}}{k_B T}\right)} \tag{S14}$$

$$f_h(E,T) = \frac{1}{1 + \exp\left(\dfrac{-\frac{\hbar^2 k_0^2}{2m_h^*} - E_{F,h}}{k_B T}\right)} = \frac{1}{1 + \exp\left(\dfrac{-\frac{m_r}{m_h^*}(E - E_g) - E_{F,h}}{k_B T}\right)} \tag{S15}$$

If we now approximate these FD distributions for the high energy tail, we find

$$f_e(E,T) \approx C_e(T) \times \exp\left(-\frac{E - E_g}{\frac{m_e^*}{m_r^*} k_B T}\right) = C_e(T) \times \exp\left(-\frac{E - E_g}{\tau_e}\right) \tag{S16}$$

$$f_h(E,T) \approx 1 - C_h(T) \times \exp\left(-\frac{E - E_g}{\frac{m_h^*}{m_r^*} k_B T}\right) = 1 - C_h(T) \times \exp\left(-\frac{E - E_g}{\tau_h}\right) \tag{S17}$$

where τ_i is defined as $\frac{m_i^*}{m_r} k_B T$ for $i = e, h$. The pre factors are defined as (although these can be seen as independent fitting parameters)

$$C_e(T) = \exp\left(\frac{E_{F,e} - E_g}{k_B T}\right) \tag{S18}$$

$$C_h(T) = \exp\left(-\frac{E_{F,h}}{k_B T}\right) \tag{S19}$$

This we can use to approximate the high energy tail of $A(E)$

$$A(E,T) = A_0(E) \times \left[1 - C_h(T) \times \exp\left(-\frac{E-E_g}{\tau_h}\right) - C_e(T) \times \exp\left(-\frac{E-E_g}{\tau_e}\right)\right] \tag{S20}$$

If we define $\Delta A(E,T) = A(E,T) - A_0(E)$, we can also find

$$\Delta A(E,T) = -A_0(E) \times \left[C_h(T) \times \exp\left(-\frac{E-E_g}{\tau_h}\right) + C_e(T) \times \exp\left(-\frac{E-E_g}{\tau_e}\right)\right] \tag{S21}$$

S3.2 Ultrafast Photo-Luminescence

We start from the idea that PL is the product of the Density of States with the FD distributions of the conduction and valence bands

$$PL(E,T) = g_{e,h}(E) \cdot f_e(E) \cdot (1 - f_h(E)) \tag{S22}$$

where $g_{e,h}(E)$ is proportional with $\sqrt{E - E_g}$, and $f_e(E,T)$ and $f_h(E,T)$ are defined as before. $(1 - f_h(E,T))$ here denotes the chance of the valence band not being occupied with an electron (so: occupied with a hole).

The same selection rule for the transition applied from before, which is

$$\hbar\omega = E = E_C(k) - E_V(k) = E_g + \frac{\hbar^2 k^2}{2m_e^*} + \frac{\hbar^2 k^2}{2m_h^*} = E_g + \frac{\hbar^2 k^2}{2m_r} \tag{S23}$$

We can solve this to k to find

$$k_0 = \sqrt{\frac{2m_r}{\hbar^2}(E - E_g)} \tag{S24}$$

for this k value, defined as k_0, a transition is allowed. We can use this in the FD distributions:

$$f_e(E,T) = \frac{1}{1 + \exp\left(\dfrac{E_g + \frac{\hbar^2 k_0^2}{2m_e^*} - E_{F,e}}{k_B T}\right)} = \frac{1}{1 + \exp\left(\dfrac{E_g + \frac{m_r}{m_e^*}(E - E_g) - E_{F,e}}{k_B T}\right)} \tag{S25}$$

$$1 - f_h(E,T) = 1 - \frac{1}{1 + \exp\left(\frac{-E_{F,h} - \frac{\hbar^2 k_0^2}{2m_h^*}}{k_B T}\right)} \tag{S26}$$

$$= 1 - \frac{1}{1 + \exp\left(\frac{-E_{F,h} - \frac{m_r}{m_h^*}(E - E_g)}{k_B T}\right)} \tag{S27}$$

$$= \frac{1 + \exp\left(\frac{-E_{F,h} - \frac{m_r}{m_h^*}(E - E_g)}{k_B T}\right) - 1}{1 + \exp\left(\frac{-E_{F,h} - \frac{m_r}{m_h^*}(E - E_g)}{k_B T}\right)} \tag{S28}$$

$$= \frac{1}{1 + \exp\left(\frac{E_{F,h} + \frac{m_r}{m_h^*}(E - E_g)}{k_B T}\right)} \tag{S29}$$

Now we can start approximating:

$$f_e(E,T) \approx C_e(T) \times \exp\left(-\frac{E - E_g}{\tau_e}\right) \tag{S30}$$

$$1 - f_h(E,T) \approx C_h(T) \times \exp\left(-\frac{E - E_g}{\tau_h}\right) \tag{S31}$$

So we finally end up with

$$PL(E,T) = C_e \cdot C_h \cdot \sqrt{E - E_g} \cdot \exp\left(-\frac{E - E_g}{\tau_e}\right) \cdot \exp\left(-\frac{E - E_g}{\tau_h}\right) \tag{S32}$$

$$= C_e \cdot C_h \cdot \sqrt{E - E_g} \cdot \exp\left(-\frac{E - E_g}{\tau_r}\right) \tag{S33}$$

where $\tau_r = \left(\frac{1}{\tau_e} + \frac{1}{\tau_h}\right)^{-1}$, which actually equals

$$\tau_r = \frac{\tau_h + \tau_e}{\tau_h \tau_e} \tag{S34}$$

$$= \frac{\frac{m_h^*}{m_r} + \frac{m_e^*}{m_r}}{\frac{m_h^*}{m_r} \cdot \frac{m_e^*}{m_r}} \times k_B T \tag{S35}$$

$$= \frac{m_h^* + m_e^*}{m_h^* \cdot m_e^*} \cdot \frac{1}{m_r} \times k_B T \tag{S36}$$

$$= k_B T \tag{S37}$$

So we obtain:

$$PL(E,T) = C_e(T) \cdot C_h(T) \times \sqrt{E - E_g} \cdot \exp\left(-\frac{E - E_g}{k_B T}\right) \tag{S38}$$

We can combine the product of the two pre factors $C(T) = C_e(T) \cdot C_h(T)$.

It is clear from this derivation that the PL case is easier to fit: the exponential simplifies to a single Boltzmann without any additional factors in the exponent, contrary to the transient absorption case.

In summary, the final expressions to use are given by:

$$PL(E,T) = C(T) \cdot \sqrt{E - E_g} \cdot \exp\left(-\frac{E - E_g}{k_B T}\right) \tag{S39}$$

and

$$\Delta A(E,T) = -A_0(E) \times \left[C_h(T) \times \exp\left(-\frac{E - E_g}{\tau_h}\right) + C_e(T) \times \exp\left(-\frac{E - E_g}{\tau_e}\right)\right] \tag{S40}$$

S3.3 C_e and C_h

Lets take another look at the constants:

$$C_e(T) = \exp\left(\frac{E_{F,e} - E_g}{k_B T}\right) \tag{S41}$$

$$C_h(T) = \exp\left(-\frac{E_{F,h}}{k_B T}\right) \tag{S42}$$

To find the relationship between these two pre factors we need to find the quasi Fermi levels:

$$E_{F,e} = k_B T \cdot F_{1/2}^{-1}\left(\frac{n}{N_{e,eff}}\right) + E_g \tag{S43}$$

$$E_{F,e} = -k_B T \cdot F_{1/2}^{-1}\left(\frac{n}{N_{h,eff}}\right) \tag{S44}$$

Where the Fermi-Dirac integral cannot be solved analytically, and $N_{i,eff}$ is given by $2\left(\frac{m_i^* k_B T}{2\pi\hbar^2}\right)^{3/2}$ but can be approximated in two regimes:

$$F_{1/2}(\eta) = \begin{cases} e^{\eta} & \eta \ll -1 \\ \frac{4}{3}\left(\frac{\eta^3}{\pi}\right)^{1/2} & \eta \gg -1 \end{cases}$$

Which each can be inverted to find

$$F_{1/2}^{-1}(\nu) = \begin{cases} \ln(\nu) & \nu \ll e^{-1} \\ \left[\frac{9\pi}{16} \cdot \nu^2\right]^{1/3} & \nu \gg e^{-1} \end{cases}$$

We can take a look at each of these cases seperately.

$\nu \gg \mathbf{e^{-1}} => \frac{\mathbf{n}}{\mathbf{N_{i,eff}}} \gg \mathbf{e^{-1}}$ The simplest case, since the logarithm and exponential cancel each other out. This holds for low carrier densities.

$$E_{F,e} = k_B T \cdot \ln\left(\frac{n}{N_{e,eff}}\right) + E_g \tag{S45}$$

$$E_{F,h} = -k_B T \cdot \ln\left(\frac{n}{N_{h,eff}}\right) \tag{S46}$$

From which we can find $C_e(T)$ and $C_h(T)$

$$C_e(T) = \exp\left(\frac{k_B T \cdot \ln\left(\frac{n}{N_{e,eff}}\right) + E_g - E_g}{k_B T}\right) \tag{S47}$$

$$= \exp\left(\ln\left(\frac{n}{N_{e,eff}}\right)\right) \tag{S48}$$

$$= \frac{n}{N_{e,eff}} \tag{S49}$$

and

$$C_h(T) = \exp\left(\frac{k_B T \cdot \ln\left(\frac{n}{N_{h,eff}}\right)}{k_B T}\right) \tag{S50}$$

$$= \exp\left(\ln\left(\frac{n}{N_{h,eff}}\right)\right) \tag{S51}$$

$$= \frac{n}{N_{h,eff}} \tag{S52}$$

Filling in the definition of $N_{i,eff}$ and dividing the two pre-factors, we get

$$\frac{C_e(T)}{C_h(T)} = \left(\frac{m_h^*}{m_e^*}\right)^{3/2} \tag{S53}$$

$\nu \ll \mathbf{e^{-1}} => \frac{\mathbf{n}}{\mathbf{N_{i,eff}}} \ll \mathbf{e^{-1}}$ Here the solution is not quite so elegant, and we are in the high density regime

$$E_{F,e} = k_B T \cdot \left[\frac{9\pi}{16}\left(\frac{n}{N_{e,eff}}\right)^2\right]^{1/3} + E_g \tag{S54}$$

$$E_{F,h} = -k_B T \cdot \left[\frac{9\pi}{16} \left(\frac{n}{N_{h,eff}} \right)^2 \right]^{1/3} \tag{S55}$$

Which we again fill in in the definition of the pre-factors

$$C_e(T) = \exp\left(\frac{k_B T \cdot \left[\frac{9\pi}{16} \left(\frac{n}{N_{e,eff}} \right)^2 \right]^{1/3} + E_g - E_g}{k_B T} \right) \tag{S56}$$

$$= \exp\left(\left[\frac{9\pi}{16} \left(\frac{n}{N_{e,eff}} \right)^2 \right]^{1/3} \right) \tag{S57}$$

$$= \exp\left(\left[\frac{9\pi}{64} \cdot n^2 \right]^{1/3} \cdot \frac{2\pi\hbar^2}{m_e^* k_B T} \right) \tag{S58}$$

and

$$C_h(T) = \exp\left(\frac{k_B T \cdot \left[\frac{9\pi}{16} \left(\frac{n}{N_{h,eff}} \right)^2 \right]^{1/3}}{k_B T} \right) \tag{S59}$$

$$= \exp\left(\left[\frac{9\pi}{16} \left(\frac{n}{N_{h,eff}} \right)^2 \right]^{1/3} \right) \tag{S60}$$

$$= \exp\left(\left[\frac{9\pi}{64} \cdot n^2 \right]^{1/3} \cdot \frac{2\pi\hbar^2}{m_h^* k_B T} \right) \tag{S61}$$

Before dividing the two pre-factors, we can define $c = \left[\frac{9\pi}{64}\right]^{1/3} \cdot \frac{2\pi\hbar^2}{k_B}$ for ease of notation. When we divide the two factors we get

$$\frac{C_e(T)}{C_h(T)} = \exp\left(c \cdot \frac{n^{2/3}}{T} \times \left[\frac{1}{m_e^*} - \frac{1}{m_h^*} \right] \right) \tag{S62}$$

Here we see that the pre-factors become temperature and carrier density dependent. Interestingly, in the limit where the effective masses become equal, this ratio becomes one, meaning the ratio of C_h and C_e becomes independent of n, T. Similarly, the denominator in

both exponentials become $2k_BT$.

We can check the limits of the different regions for both electrons and holes. The limit is

$$\frac{n_{thr}}{N_{i,eff}} \approx e^{-1} \tag{S63}$$

which we can rewrite as

$$n_{thr} = e^{-1} \cdot 2 \left(\frac{m_i^* k_B T}{2\pi\hbar^2} \right)^{3/2} \tag{S64}$$

We can calculate this limit for both the electrons and holes. Due to the typically higher mass of the holes, the threshold density will be higher and as such the independence will work for larger carrier densities for C_V than for C_C. Of course, for the actual temperature fit, the constant ratio will hold only up until one of the two pre-factors become carrier density dependent.

These results can be summarised in Figure S7. (a) shows the exact ratio (full lines) and the two approximations (constant low limit, which is around 6.5, and coloured dashed lines for the high limit). (b) shows the change in threshold carrier density in function of temperature for electrons (red), holes (blue) and also the crossing point between low and high limit (black). The latter case is when the two limits equal each other. In general we can conclude here that for a reasonable carrier density ($n = 10^{20}$ cm^{-1} is about the maximum) the lower limit applies. Using this approximation, we can rewrite ΔA

$$\Delta A(E,T) = -A_0(E) \cdot C(T) \times \left[(m_e^*)^{3/2} \times \exp\left(-\frac{E - E_g}{\tau_h} \right) + (m_h^*)^{3/2} \times \exp\left(-\frac{E - E_g}{\tau_e} \right) \right] \tag{S65}$$

The pre-factor only gives part of the image, since the slopes of both the electron and hole exponentials will be scaled according to the τ_i factor. For the case that $m_e^* \ll m_h^*$, we can see that the electron exponential will decay much quicker although it has a higher weight. This can be seen in Figure S8, where the sum of exponentials is shown and it is clear that there are two different regimes. For this specific case, it can be seen that mostly the hole

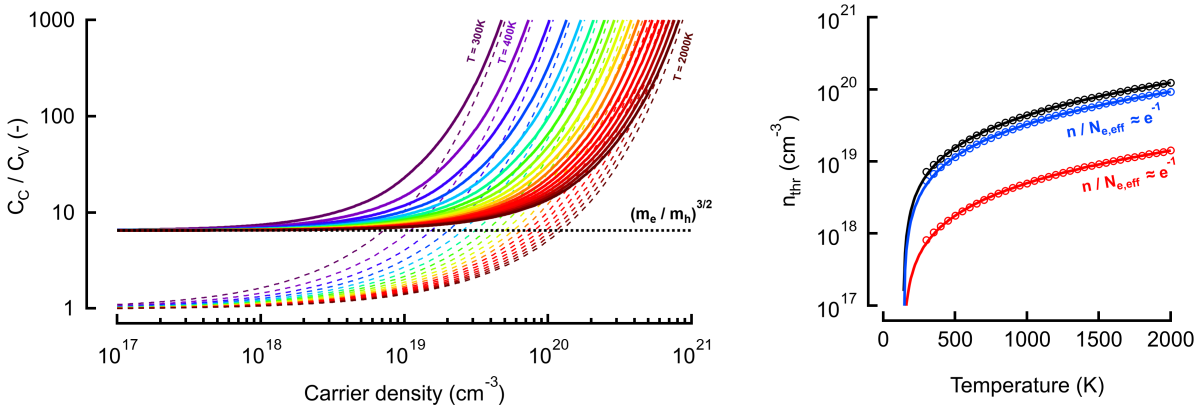

Figure S7: (a) Ratio of the pre-factors of the two exponentials derived from the TA temperature fitting. (b) the threshold for the two regimes in function of the temperature.

exponential will in fact be relevant in our fitting region, despite its lower weight. For the general case we can look at the tipping point E_{thr} where the two exponentials become equal to each other (and as such for energies higher than this value the hole exponential will be the dominant decay):

$$C_e(T) \times \exp\left(-\frac{E_{thr} - E_g}{\tau_e}\right) = C_h(T) \times \exp\left(-\frac{E_{thr} - E_g}{\tau_h}\right) \tag{S66}$$

This can be solved for E_{thr}

$$E_{thr} = E_g + \frac{m_h^* + m_e^*}{m_h^* - m_e^*} \cdot kT \times \ln\left(\frac{C_e(T)}{C_h(T)}\right) \tag{S67}$$

Which will only depend linearly on the temperature for the low density regime

$$E_{thr} = E_g + \frac{m_h^* + m_e^*}{m_h^* - m_e^*} \cdot kT \times \frac{3}{2} \cdot \ln\left(\frac{m_h^*}{m_e^*}\right) \tag{S68}$$

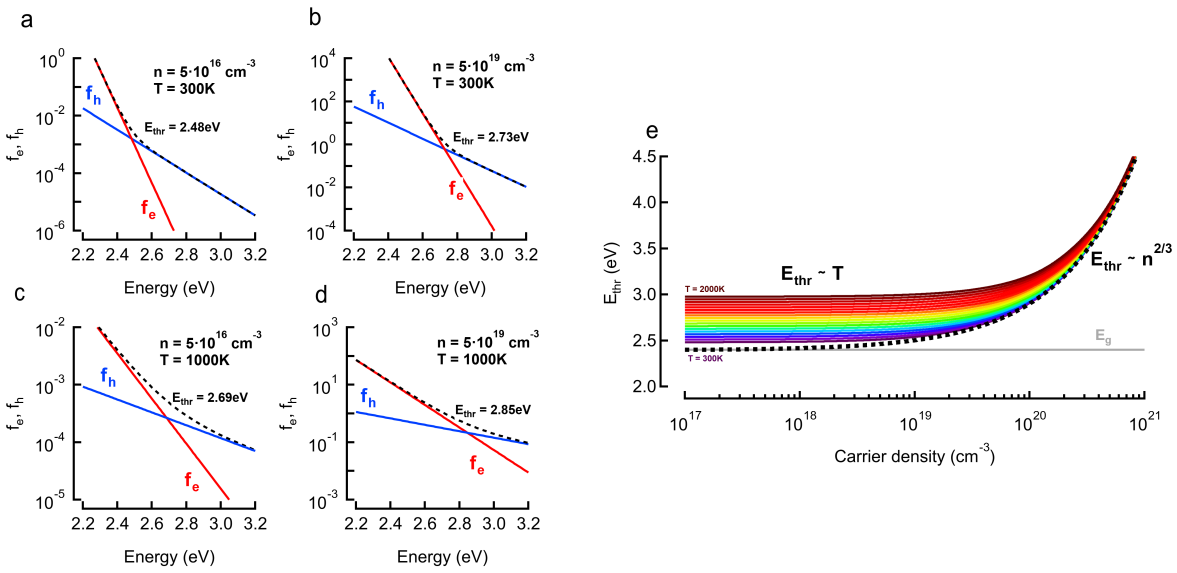

Figure S8: (a)-(d) magnitude of each of the exponentials for 4 different combinations, low/high temperature and carrier density. (e) E_{thr} in function off the carrier density and plotted for a range of temperatures. The dotted line shows the high density limit.

and will become temperature independent for the high density regime

$$E_{thr} = E_g + \frac{m_h^* + m_e^*}{m_h^* - m_e^*} \cdot kT \times \left(c \cdot \frac{n^{2/3}}{T} \times \left[\frac{1}{m_e^*} - \frac{1}{m_h^*} \right] \right) \tag{S69}$$

$$= E_g + \left(\frac{9\pi}{64} \right)^{1/3} \cdot \frac{2\pi\hbar^2}{m_r} \cdot n^{2/3} \tag{S70}$$

As long as we have moderate densities and temperatures, we can see from Figure S8 that the hole exponential will be dominant. Or putting it differently: if we choose the lower limit well (high enough) then we can fit the TA data with a single exponential. Interestingly, the low carrier regime effect also scaled with the difference between the effective masses of electrons and holes, so if they become equal the effect dissapears. This means that for equal masses and low carrier densities, you can start fitting from the bandgap energy.

References

1. Baranov, D.; Toso, S.; Imran, M.; Manna, L. Investigation into the Photoluminescence Red Shift in Cesium Lead Bromide Nanocrystal Superlattices. *The Journal of Physical Chemistry Letters* **2019**, *10*, 655–660.

2. Tanghe, I.; Samoli, M.; Wagner, I.; Cayan, S.; Khan, A. H.; Chen, K.; Hodgkiss, J.; Moreels, I.; Van Thourhout, D.; Hens, Z.; Geiregat, P. Disruptive Optical Gain from Bulk CdS Nanocrystals through Giant Band Gap Renormalization. *Nature Nanotechnology* **2023**, *Accepted for publication*.

3. Maes, J.; Balcaen, L.; Drijvers, E.; Zhao, Q.; De Roo, J.; Vantomme, A.; Vanhaecke, F.; Geiregat, P.; Hens, Z. Light Absorption Coefficient of CsPbBr 3 Perovskite Nanocrystals. *The Journal of Physical Chemistry Letters* **2018**, *9*, 3093–3097.

4. Hens, Z.; Moreels, I. Light absorption by colloidal semiconductor quantum dots. *Journal of Materials Chemistry* **2012**, *22*, 10406–10406.

5. Chen, K.; Gallaher, J. K.; Barker, A. J.; Hodgkiss, J. M. Transient grating photoluminescence spectroscopy: An ultrafast method of gating broadband spectra. *Journal of Physical Chemistry Letters* **2014**, *5*, 1732–1737.